Rika Rosnelly

Diperiksa : Lppm Universitas Potensi Utama

Submission date: 11-Feb-2019 02:43PM (UTC+0700)
Submission ID: 1076273499
File name: of_Malaria_Parasite_and_Its_Life-Cycle-Stages_in_Blood_Smear.pdf (1.01M)
Word count: 4003
Character count: 20054

Performance of SVM and ANFIS for Classification of Malaria Parasite and Its Life-Cycle-Stages in Blood Smear

Sri Hartati[1(✉)], Agus Harjoko[1], Rika Rosnelly[2], Ika Chandradewi[1], and Faizah[1]

[1] Universitas Gadjah Mada, Sekip Utara, Yogyakarta 55281, Indonesia
shartati@ugm.ac.id
[2] Department of Informatics, University of Potensi Utama, Medan, Indonesia

Abstract. A method to classify Plasmodium malaria disease along with its life stage is presented. The geometry and texture features are used as Plasmodium features for classification. The geometry features are area and perimeters. The texture features are computed from GLCM matrices. The support vector machine (SVM) classifier is employed for classifying the Plasmodium and its life stage into 12 classes. Experiments were conducted using 600 images of blood samples. The SVM with RBF kernel yields an accuracy of 99.1%, while the ANFIS gives an accuracy of 88.5%.

Keywords: Malaria · Geometry · Texture · GLCM · RBF

1 Introduction

Malaria is a highly hazardous disease to humans because it can cause death. Malaria is caused by parasites which are transmitted by the female Anopheles mosquito. These mosquitoes bite infected Plasmodium from a person previously infected with the parasite. Plasmodium is divided into four types: Plasmodium ovale, Plasmodium malaria, Plasmodium falciparum, and Plasmodium vivax. Plasmodium vivax is often found in patients with malaria disease. Plasmodium falciparum is the cause of deaths of nearly 90% of the patient with malaria disease in the world.

Microscopic examination is required to determine the parasite Plasmodium visually by identifying directly at the patient's blood dosage. The microscopic examination result is highly dependent on the expertise of the laboratory worker (health analyst) that identifies the parasite Plasmodium. The microscopic examination technique is the gold standard for the diagnosis of malaria. Among some techniques which can be used for malaria diagnosis the peripheral blood smear (PBS), quantitative buffy coat (QBC), rapid diagnosis test (RDT), Polymerase Chain Reaction (PCR), and Third Harmonic Generation (THG) [1, 2]. The PBS technique is the most widely used malaria diagnosis even though has limitations of human resistance due to the time required.

To diagnose malaria parasite, a manual calculation process that uses a microscopic examination of Giemsa-stained thick and thin blood smears is carried out. This process

B. W. Yap et al. (Eds.): SCDS 2018, CCIS 937, pp. 110–121, 2019.
https://doi.org/10.1007/978-981-13-3441-2_9

requires a long time and is a tedious process. It is very susceptible to the capabilities and skills of technicians. Its potential for mistakes made by humans is significant [3].

As an illustration, a trained technician requires about 15 min to count 100 cells. Worldwide, technicians have to deal with millions of patients every year [4]. To overcome a long and tedious process, several studies have been conducted to develop automated microscopic blood cell analysis. Some early studies showed limited performance, which leads to classifying the types of parasites present in blood cells but has not been able to show the entire stage of malaria life [5]. Similar studies were conducted with various methods to increase the accuracy of identification of infectious parasites, mainly only identifying 2–4 Plasmodium parasites that can infect humans [6]. Without specifying the life stages of malarial parasites, whereas each parasite has three different life stages, namely trophozoite, schizoite, and gametocytes [3]. Therefore, the study of the classification of the life stages of malarial parasites poses a challenge to the study [7], and successfully detects three stages of the Plasmodium parasite while in the human host, trophozoite, schizont, and Plasmodium falciparum gametocytes, even though it has not been able to detect other species. Plasmodium that can form human infection has four species: falciparum, vivax, ovale, and malaria. Each species is divided into four distinct phases, which are generally distinguishable: rings, trophozoites, schizonts, and gametocytes, so that there are sixteen different classes. This paper discusses methods for classifying 12 classes that include three types of Plasmodium and each with four life stages.

2 Data Collections

A total of 600 malaria image data of Giemsa - stained thin blood smears is obtained from Bina Medical Support Services (BPPM) in Jakarta. The malaria image data size is 2560 $\times$ 1920 pixels. The manual plasmodium classification is carried out by laboratory workers of the parasitology Health Laboratory of the North Sumatra Province, Indonesia, which provide the ground truth for the proposed method. Each image is given a label associated with the name of the parasite, i.e., Plasmodium malaria, Plasmodium falciparum, Plasmodium vivax) along with its life-cycle-stage (ring, trophozoite, schizont, or gametocyte). None of the 600 image data consist of Plasmodium ovale. Therefore the 600 image data consist of 12 classes. Figure 1 shows different Plasmodium, and their life-stages.

3 Method

The classification process of the malaria parasite is shown in Fig. 2. A blood smear is performed on the blood sample. The region of interest (ROI) is then determined to locate the area, which contains parasite. Next, three basic image processing steps are carried out, that is, preprocessing, segmentation, and feature extraction. Following that, the image classification and detection of infected red blood cells (RBC), that is called parasitemia, are carried out. In this work, the malaria images consist of three types of

Plasmodium and each has four different life stages, i.e., ring, schizont, trophozoite, and gametocyte stages.

3.1 Preprocessing

The aim of the preprocessing step is to obtain images with lower noise and higher contrast than the original images for further processing. Blood smear images might be affected by the illumination and color distribution of blood images due to the camera setting and staining variability. Most of the microscopes yield blood cells with quite similar colors. Therefore, image enhancement and noise reduction operations are required. Low intensities of light might decrease the contrast of blood image [8]. Therefore the contrast image has to be improved using a contrast enhancement method.

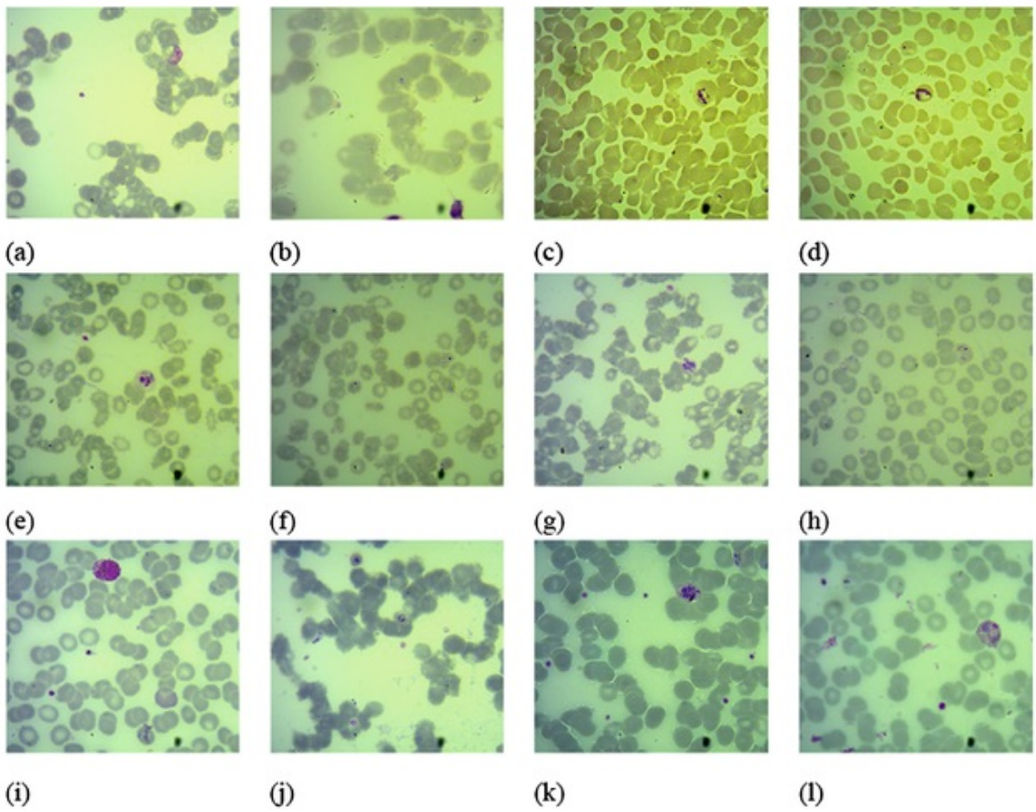

Fig. 1. Plasmodium and their life stage. (a) Falcifarum, gametocyte stage (b) Falcifarum, ring stage (c) Falcifarum, schizont stage (d) Falcifarum, trophozoite stage (e) Malariae, gametocyte stage (f) Malariae, ring stage (g) Malariae, schizont stage (h) Malariae, trophozoite stage (i) Vivax, gametocyte stage (j) Vivax, ring stage (k) Vivax, schizont stage (l) Vivax, trophozoite stage.

After image enhancement is performed, the region of interest (ROI) is carried out by manually cropping the infected RBC, because the image contains infected not only

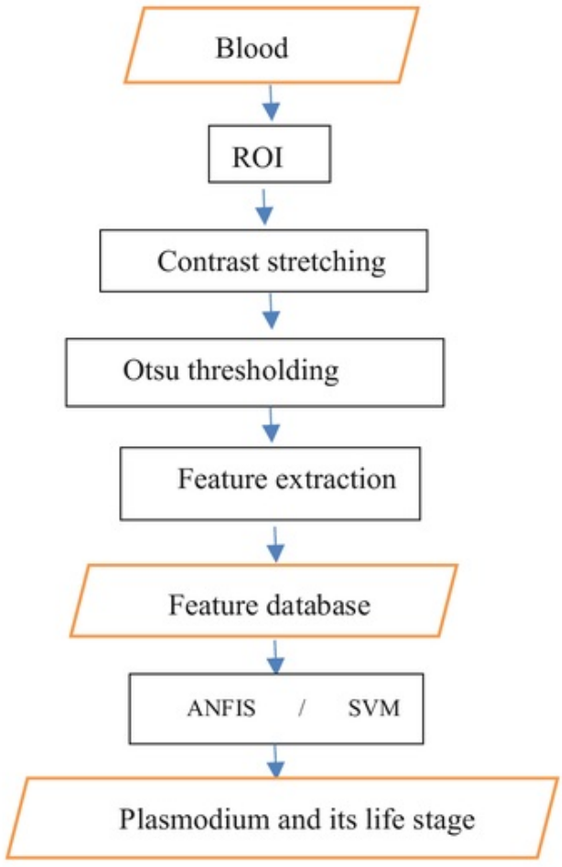

Fig. 2. Detection of the malaria parasite and its life stage.

red blood cells but also normal red blood cells, white blood cells, platelets, and artifacts. Experts validate the process of determining ROI. Experience indicates that the appropriate size for ROI is 256×256 pixels. These preprocessing produces an image with good contrast.

3.2 Segmentation

Segmentation attempts to subdivide an image into sub-images or segments such that each segment fulfills certain characteristics. In this case, as the malaria parasite affects the red blood cells, the segmentation is carried out to separate red blood cells from the rest, and the result is the red blood cells in the microscopic images of the blood sample. Initially, the RGB image of ROI is converted into the gray image since the red blood cells can be distinguished from the rest of its gray level value. In this research, Otsu's thresholding method is used for its ability to determine threshold automatically. An example is depicted in Fig. 3.

After thresholding, the morphological closing and opening are performed to extract the hole inside the infected cell and eliminate the unwanted artifacts [9]. These segmented cells are further processed and then the infected red blood cells are identified.

3.3 Features Extraction

Many studies concerning the analysis of red blood cells recently use texture features [5, 9], and color features [10, 11], to differentiate normal cells and infected cells. In this research texture and geometry, features are used. Geometry features are selected for analyzing blood since hematologist uses these features. The selected geometric features are area and perimeter. The area is defined as the number of pixels of the object that indicates the size of the object and is calculated using

$$\text{Area} = \sum_x \sum_y f(x, y). \tag{1}$$

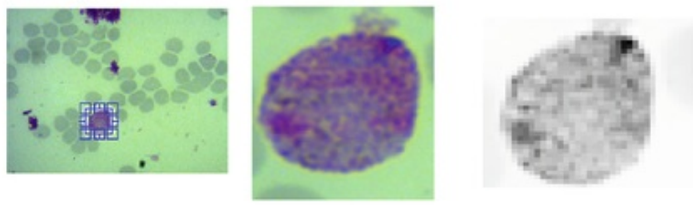

(a) (b) (c)

Fig. 3. (a) Initial image, (b) Region of Interest (ROI) (c) grayscale of ROI.

The perimeter is expressed as the continuous line forming the boundary of a closed geometric object. It can be calculated as

$$Perimeter = \sum_x \sum_y \begin{matrix} f(x,y), \\ x,y \in Boundary\ region \end{matrix} \tag{2}$$

The texture features are computed from the Gray-Level Co-occurrence Matrix (GLCM) of the ROI image. The GLCM is used to calculate the co-occurrence of a pair of pixels with gray-level value and in a particular direction. A GLCM element Pθ, d(i, j) is the joint probability of the gray level pairs *i* and *j* in a given direction θ separated by a distance of d units. In this research, the GLCM features are extracted using one distance (d = {1}), and three directions (θ = {45°, 90°, 135°}). These texture based features can be calculated as follows:

1. *Contrast* is the measure of intensity contrast between a pixel and the neighboring pixel over the complete image.

$$\sum_{i,j}^{N-1} p_{i,j}(i-j)^2 \tag{3}$$

2. *Entropy*
   Entropy is the measure of the complexity of the image, and it represents the amount of information contained in data distribution. The higher the entropy value, the higher the complexity of the image.

$$\sum_{i,j}^{N-1} p_{i,j}(-\ln p_{i,j})^2 \tag{4}$$

3. *Energy*
   Energy is a measure of the pixel intensities in grayscale value. Energy is computed by summing all squared elements in the GLCM matrix,

$$\sum_{i,j}^{n-1} {p_{i,j}}^2 \tag{5}$$

4. Homogeneity is the measure of the homogeneity of a particular region. This value is high when all pixels have the same values or uniform.

$$\sum_{i,j=0}^{N-1} \frac{p_{i,j}}{1+(i-1)^2} \tag{6}$$

5. Correlation indicates how a pixel is correlated with the neighboring pixels in a particular area

$$\sum_{i,j=0}^{N-1} p_{i,j} \left[\frac{(i-\mu_i)(i-\mu_j)}{\sqrt{\sigma_i^2 \sigma_j^2}} \right] \tag{7}$$

3.4 Classification Using ANFIS

A specific approach in neuro-fuzzy development is the adaptive neuro-fuzzy inference system (ANFIS), which has shown significant results in modeling nonlinear functions. The ANFIS learn features in the data set and adjusts the system parameters according to a given error criterion. In this research, the ANFIS is a fuzzy Sugeno model. To present the ANFIS architecture, fuzzy if-then rules based on a first-order Sugeno model are considered. The output of each rule can be a linear combination of input variables and a constant term or can be only a constant term. The final output is the weighted average of each rule's output. Basic architecture with two inputs x and y and one output z is shown in Fig. 4.

Suppose that the rule base contains two fuzzy if-then rules of

Rule 1: If x is A_1 and y is B_1, then $f_1 = p_1x + q_1y + r_1$,
Rule 2: If x is A_2 and y is B_2, then $f_2 = p_2x + q_2y + r_2$.

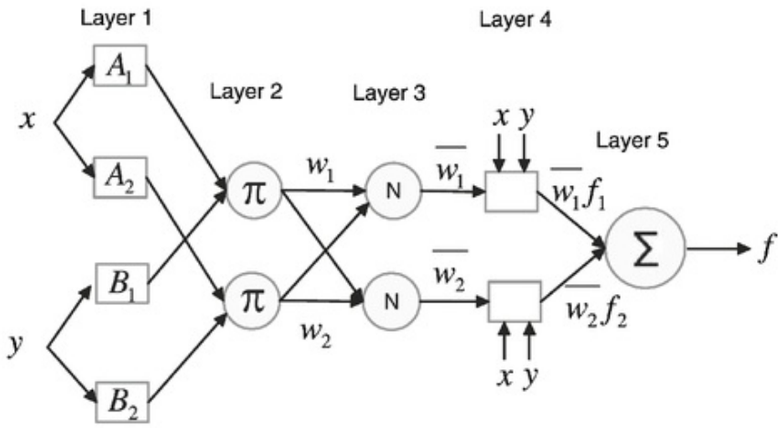

Fig. 4. The architecture of ANFIS.

Layer 1: Every node i in this layer is an adaptive node with a node function

$$O_i = \mu_{A_i} \tag{8}$$

where x is the input to node i, and A_i is the linguistic label (small, large, etc.) associated with this node function. In other words, Eq. (8) is the membership function of specifies the degree to which the given x satisfies the quantifier A_i. Usually, it equals to 1 and minimum equal to 0, such as choose $\mu_{Ai}(x)$ to be bell-shaped with maximum

$$\mu_{A_i}(x) = \frac{1}{1 + \left[\left(\frac{x - x_i}{a_i}\right)^2\right]} \tag{9}$$

$$\mu_{A_i}(x) = e^{\left\{-\left(\frac{x-x_i}{a_i}\right)^2\right\}} \tag{10}$$

where a_i is the parameter set. As the values of these parameters change, the bell-shaped functions vary accordingly, thus exhibiting various forms of membership functions on linguistic label A_i. In fact, any continuous and piecewise differential functions, such as trapezoidal or triangular shaped membership functions, can also be used for node functions in this layer. Parameters in this layer are referred to as premise parameters.

Layer 2: Every node in this layer is a fixed node labeled Π which multiplies the incoming signals and sends the product out. For instance,

$$w_i = \mu_{A_i}(x) + \mu_{B_i}(y), \; i \leq 2 \tag{11}$$

Each node output represents the firing strength of a rule.

Layer 3: Every node in this layer is a circle node labeled N. The i^{th} node calculates the ratio of i to the sum of all rules firing strengths. For convenience, outputs of this layer will be called as normalized firing strengths

$$\bar{w}_i = \frac{w_i}{w_1 + w_2} \tag{12}$$

Layer 4: Every node i in this layer is a square node with a node function

$$O_i = \bar{w}_i f_1 = \bar{w}_i (p_1 x + q_1 y + r_1) \tag{13}$$

where w_i is the output of layer 3, and $\{p_1, q_1, r_1\}$ parameter set. Parameters in this layer will be referred to consequent parameters.

Layer 5: The single node in this layer is a circle node labeled as $\sum$ that computes the overall output as the summation of all incoming signals, i.e.

$$O_i = \sum_i \bar{w}_i f_1 = \frac{\sum_i w_i f_i}{\sum_i w_i} \tag{14}$$

Learning Algorithm

In the ANFIS structure, it is noticed that given the values of premise parameters, the final output can be expressed as a linear combination of the consequent parameters. The output f can be written as

$$\mathrm{f} = \frac{\mathrm{w}_1}{\mathrm{w}_1 + \mathrm{w}_2}\mathrm{f}_1 + \frac{\mathrm{w}_2}{\mathrm{w}_1 + \mathrm{w}_2}\mathrm{f}_2 \tag{15}$$

$$\mathrm{w}_1 f_1 + \mathrm{w}_2 f_2 = (\overline{w_1} x)p_1 + (\overline{w_1} x)q_1 + (\overline{w_1} x)r_1 + (\overline{w_2} x)p_2 + (\overline{w_2} x)q_2 + (\overline{w_2} x)r_2 \mathrm{w}_1 \mathrm{w}_2$$

where f is linear in the consequent parameters (p_1, q_1, r_1, p_2, q_2, r_2). In the feedforward learning process, consequent parameters are identified by the least squares estimate. In the backward learning process, the error signals, which are the derivatives of the squared error with respect to each node output, propagate backward from the output layer to the input layer. In this backward pass, the premise parameters are updated by the gradient descent algorithm.

3.5 Classification Using SVM

Support Vector Machines (SVMs) are state-of-the-art classification methods based on machine learning theory [12]. Compared with other methods such as artificial neural networks, decision trees, and Bayesian networks, SVMs have significant advantages because of their high accuracy, elegant mathematical tractability, and direct geometric interpretation. Besides, they do not need a large number of training samples to avoid overfitting. The support vector machine (SVM) is selected to classify the Plasmodium type along with its life stage. There are 12 possible classes since there are three types of Plasmodium and four life stages. Two different kernels are implemented, and their performances are compared.

Before the SVM is used for classification, it is trained using training data. In the process of training, the SVM uses feature matrix, as the training input, which is obtained in the features extraction process. The training data classification process is to seek support vector and bias of input data. The following is the training algorithm for each binary SVM:

Input: Z is a matrix of Plasmodium features obtained from feature extraction process. Output: Strain vector as a target. Y_{train} vector is a column vector for classification of the first class, where all images of blood preparations of the first class will be symbolized by number 1, all images of blood smears from other classes with number −1. In this study, a Gaussian kernel function with variance (σ) = one is used. The next step is to calculate Hessian matrix, i.e., multiplication of a Gaussian kernel with Y_{train}. Y_{train} is a vector that contains values of 1 and −1. Hessian matrix is later used as input variables in quadratic programming. The training steps are described as follows:

1. Determine input ($Z = X_{train}$) and Target (Y_{train}) as a pair of training from two classes.
2. Calculating Gaussian kernel

$$K(Z, Z_i) = \exp\left(\frac{-|Z - Z_i|^2}{2\sigma^2}\right) \tag{16}$$

3. Calculate Hessian matrix

$$H = K(Z, Z_i) * Y * YT \tag{17}$$

Assign c and *epsilon*. The term c is a constant in Lagrangian multipliers and epsilon (cost parameter) is the upper limit value of α, which serves to control classification error. This study used value of $c = 100000$ and $epsilon = 1 \times 10^{-7}$.

4. Assign vector e as a unit vector which has the same dimension with the dimension of Y.
5. Calculating quadratic programming solutions

$$L(\alpha) = \frac{1}{2}\alpha^{+} H\alpha + e^{T}\alpha \tag{18}$$

In testing process, data that have never been used for training are used. Results of this process are an index value of the largest decision function, stating the class of the testing data. If a class in the classification test match the test data classes, classification is stated to be correct. The final result of classification is an image of blood that matches with an index value of decision function using SVM one against all.

Having an input data feature vector T for test data (w, x, b), and k number of classes, the input data then is used for the testing process. The input is generated in the process of feature extraction, The process of testing is as follows:

1. Calculate Kernel Gaussian

$$K(T, x_i) = \exp\left(\frac{-|T - x_i|^2}{2\sigma^2}\right) \tag{19}$$

2. Calculate

$$f_i = K(T, x_i)w_i + b_i \tag{20}$$

3. Repeat steps 1, 2 for $i = 1$ to k.
4. Determining the maximum value of f_i
5. A class i is a class from T which has the largest value of f_i

The performance of both the proposed method is measured regarding accuracy, sensitivity, and specificity. The true positive (TP) shows the image of blood smears correctly identified. False positive (FP) is the image of Plasmodium classified incorrectly. The true negative (TN) indicates the number of images that is not a member of a class and is correctly identified as not a member of class (NV). False negative (FN) showed the number image of blood smears that should not be members of class but identified as a member of class.

$$\begin{aligned} \text{Accuracy} &= (\text{TP} + \text{TN})/(\text{TP} + \text{TN} + \text{FP} + \text{FN}), \\ \text{Sensitivity} &= \text{TP}/(\text{TP} + \text{FN}), \\ \text{Specificity} &= \text{TN}/(\text{FP} + \text{TN}) \end{aligned}$$

4 Experimental Results

Experiments were conducted to evaluate the performance of the proposed classification method. A total of 600 image data from Bina Medical Support Services (BPPM), Jakarta, Indonesia were used. The resolution of the image is 2560 × 1920 pixels. Parasite labeling was carried out by a professional from a parasitology health laboratory in North Sumatra, Indonesia. There are three types of parasites, i.e., Plasmodium malariae, Plasmodium falciparum, and Plasmodium vivax. Each plasmodium is distinguished into four life stages, i.e., ring, trophozoite, schizont, or gametocyte.

The ANFIS neural network is used for classifying the Plasmodium type along with its life stages which makes a total combination of 12 classes. The testing process utilizes k-fold cross-validation model were adopted with k = 1, 2, 3, 4, 5. Table 1 shows the experimental results for the algorithm.

Table 1. Experimental results for ANFIS algorithm.

	K = 1	K = 2	K = 3	K = 4	K = 5
Accuracy (%)	89.29	84.82	90.62	91.07	86.74
Precision (%)	89.30	83.28	90.62	92.10	86.65
Sensitivity (%)	89.31	98.00	90.62	89.60	85.86
Specificity (%)	89.32	86.30	90.62	91.00	88.33

As seen in Table 1, the ANFIS gives an average accuracy of 88,503%. While as seen in Table 2, the SVM with linear kernel gives an average accuracy of 57% which is not satisfactory. The highest accuracy, which is 62%, was obtained when k = 3. As shown in Table 3, SVM with RBF kernel yields a much better results with an average accuracy of 99.1%.

Table 2. Experimental results for SVM classifier with linear kernel.

	K = 1	K = 2	K = 3	K = 4	K = 5
Accuracy (%)	53.0	52.0	62.0	60.0	56.0
Precision (%)	33.0	34.4	45.3	37.8	44.0
Sensitivity (%)	38.9	37.4	45.4	44.1	43.4
Specificity (%)	95.4	95.6	95.5	96.3	95.7

Table 3. Experimental results for SVM classifier with RBF kernel.

	K = 1	K = 2	K = 3	K = 4	K = 5
Accuracy (%)	100	98.0	100	100	98.0
Precision (%)	100	96.2	100	100	97.9
Sensitivity (%)	100	99.1	100	100	97.0
Specificity (%)	100	99.8	100	100	99.8

5 Conclusion

A method to classify plasmodium of malaria disease along with its life stage is presented. The geometry and texture features are used for classification. The texture features are computed from GLCM matrices. The SVM classifier is employed for classifying the Plasmodium and its life stage into 12 classes. The SVM with linear kernel gives the accuracy of 57%; the ANFIS gives an accuracy of 88.5% whereas SVM with RBF kernel yields an accuracy of 99.1%.

Acknowledgment. The authors would like to thank the Directorate General of Higher Education, the Ministry of Research and Higher Education of the Republic of Indonesia for sponsoring this research. The authors would also like to thank the parasitology Health Laboratory of the North Sumatra Province and Bina Medical Support Services (BPPM), Jakarta, for supporting this research.

References

1. World Health Organization: Basic Malaria Microscopy, Part I Learners Guide, 2nd edn. World Health Organization, Geneve (2010). https://doi.org/10.1016/0169-4758(92)90107-D
2. Jain, P., Chakma, B., Patra, S., Goswami, P.: Potential biomarkers and their applications for rapid and reliable detection of malaria. BioMed Res. Int., 201–221 (2014). https://doi.org/10.1155/2014/852645
3. McKenzie, F.E.: Dependence of malaria detection and species diagnosis by microscopy on parasite density. Am. J. Trop. Med. Hyg. **69**(4), 372–376 (2003)
4. Tek, F.B., Dempster, A.G., Kale, I.: Malaria parasite detection in peripheral blood images. In: 17th International Conference British Machine Vision Conference Proceedings, pp. 347–356. British Machine Vision Association, Edinburgh (2006). https://doi.org/10.1109/ACCESS.2017.2705642
5. Ross, N.E., Pittchard, C.J., Rubbin, D.M., Duse, A.G.: Automated image processing method for the diagnosis and classification of malaria on thin blood smears. Med. Biol. Eng. Comput. **44**(5), 427–436 (2006). https://doi.org/10.1109/ICSIPA.2013.6708035
6. Komagal, E., Kumar, K.S., Vigneswaran, A.: Recognition and classification of malaria plasmodium diagnosis. Int. J. Eng. Res. Technol. **2**(1), 1–4 (2013)
7. Nugroho, H.A., Akbar, S.A., Muhandarwari, E.E.H.: Feature extraction and classification for detection malaria parasites in thin blood smear. In: 2nd International Conference on Information Technology, Computer, and Electrical Engineering Proceedings, pp. 198–201. IEEE, Semarang (2015). https://doi.org/10.1109/ICITACEE.2015.7437798

8. Khatri, E.K.M., Ratnaparkhe, V.R., Agrawal, S.S., Bhalchandra, A.S.: Image processing approach for malaria parasite identification. Int. J. Comput. Appl. 5–7 (2014)
9. Kumar, A., Choudhary, A., Tembhare, P.U., Pote, C.R.: Enhanced identification of malarial infected objects using Otsu algorithm from thin smear digital images. Int. J. Latest Res. Sci. Technol. **1**(159), 2278–5299 (2012)
10. Ahirwar, N., Pattnaik, S., Acharya, B.: Advanced image analysis based system for automatic detection and classification of malaria parasite in blood images. Int. J. Inf. Technol. Knowl. Manag. **5**(1), 59–64 (2012)
11. Chen, T., Zhang, Y., Wang, C., Ou, Z., Wang, F., Mahmood, T.S.: Complex local phase based subjective surfaces (CLAPSS) and its application to DIC red blood cell image segmentation. J. Neurocomputing **99**, 98–110 (2013). https://doi.org/10.1016/j.neucom.2012.06.015
12. Bhavsar, T.H., Panchal, M.H.: A review on support vector machine for data classification. Int. J. Adv. Res. Comput. Eng. Technol. **1**(10), 185–189 (2012)

Bu Rika

ORIGINALITY REPORT

12%	9%	11%	0%
SIMILARITY INDEX	INTERNET SOURCES	PUBLICATIONS	STUDENT PAPERS

MATCH ALL SOURCES (ONLY SELECTED SOURCE PRINTED)

1%

★ Reem Sabah, Raja N. Ainon. "Isolated Digit Speech Recognition in Malay Language Using Neuro-Fuzzy Approach", 2009 Third Asia International Conference on Modelling & Simulation, 2009

Publication

Exclude quotes	On	Exclude matches	< 1%
Exclude bibliography	On		